Electronic Supporting Information (ESI)

Isostructural Functionalization by –OH and –NH_2: Different Contributions to CO_2 Adsorption

Zhiyong Lu,[a]* Yue Xing, Liting Du,[b] Haiyan He,[a] Jianfeng Zhang[a]*, Cheng Hang[c]

a. *College of Mechanics and Materials, Hohai University, Nanjing 210098, China.*
Email: johnlook1987@gmail.com; jfzhang_sic@163.com
b. *Advanced Analysis and Testing Center, Nanjing Forestry University, Nanjing 210037, China.*
c. *State Key Laboratory of Coordination Chemistry, Nanjing University, Nanjing 210093, China.*

1. Preparation of 1,3-bis(3,5-dicarboxylphenyl)-benzene (H_4BDPB).

Into a flask flushed with N_2, 1,3-dibromobenzene (0.71 g, 3 mmol), 3,5-diethyllisophalate-5-boronic acid (1.84 g, 7.8 mmol), saturated sodium bicarbonate solution (10 ml) were placed and 40 mL of 1,4-dioxane was added. Tetrakis(triphenylphosphine)palladium(0) (0.466 g, 0.404 mmol) was added to the reaction mixture with stirring, and heated to 80°C for 12 hours. The resultant mixture poured into water (100 mL), extracted with CH_2Cl_2, and dried over $MgSO_4$. The volatiles were removed by evaporation under reduced pressure, and the solid residue was purified by column chromatography to give white solid product of 3,5-bis(3,5-dicarboxylesterphenyl) benzene with the yield of 54.6 % (0.85g). A sample of potassium hydroxide (0.63 g, 11.25 mmol) was dissolved in tetrahydrofuran/water (v/v=1:1; 60 mL). To this was added 3,5-bis(3,5-dicarboxyelesterphenyl) benzene (0.85 g, 1.64 mmol), after which the solution was stirred for 24 hours at 80°C. The volatiles were removed by evaporation under reduced pressure. The residue dissolved in 20 mL of water was acidified to pH~2-3 using 1.0M HCl and stirred for 3 hours. The white precipitate was separated by filtration, washed with water, and freeze-dried. Yield=0.6 g (90.1%). ^{1}H NMR (500 MHz, DMSO-d_6, δ ppm): 13.56 (brs, 4H, COO$\underline{H}$), 8.51 (s, 2H, Ar$\underline{H}$), 8.47 (s, 4H, Ar$\underline{H}$), 8.05 (s, 1H, Ar$\underline{H}$), 7.81 (d, *J*=5Hz, 2H, Ar$\underline{H}$), 7.68 (d, *J*=5Hz, 1H, Ar$\underline{H}$). IR (KBr, cm^{-1}): 2991, 1700, 1599, 1440, 1234, 905, 755, 675, 633。

2. Preparation of 5-amino-1,3-bis(3,5-dicarboxylphenyl)-benzene (H_4ABDPB). This was synthesized by following a similar procedure to the synthesis of H_4BDPB. Excepting for changing the starting materials of 1,3-dibromobenzene to 3,5-dibromobenzenamine, the molar ratio of the reactants remained the same. ^{1}H NMR (500 MHz, DMSO-d_6, δ ppm): 13.37 (brs, 4H, COO$\underline{H}$), 8.47 (s, 2H, Ar$\underline{H}$), 8.42 (s, 4H, Ar$\underline{H}$), 7.19 (s, 1H, Ar$\underline{H}$), 7.04 (s, 2H, Ar$\underline{H}$), 5.76 (brs, 2H, N$\underline{H}$). IR (KBr, cm^{-1}): 3399, 2921, 1702, 1599, 1380, 1236, 909, 866, 760, 675, 639。

3. Preparation of 5-hydroxylic-1,3-bis(3,5-dicarboxylphenyl)-benzene (H_4OBDPB). This was synthesized by following a similar procedure to the synthesis of H_4BDPB. Excepting for changing the starting materials of 1,3-dibromobenzene to 3,5-dibromophenol, the molar ratio of the reactants remained the same. ^{1}H NMR (500 MHz, DMSO-d_6, δ ppm): 13.40 (brs, 5H, COOH), 8.53 (s, 6H, Ar$\underline{H}$), 8.37 (s, 1H, Ar$\underline{H}$), 8.27 (s, 2H, Ar$\underline{H}$). IR (KBr, cm^{-1}): 2977, 1704, 1599, 1426, 1239, 1092, 890, 756, 672。

4. X-ray collection and structure determination

Single crystal suitable for X-ray structure determination were selected and sealed in a capillary under a microscope. The X-ray diffraction intensity data were measured on a BRUKER D8 VENTURE PHOTON diffractometer at room temperature using graphite monochromated Mo/Kα radiation (λ = 0.71073 Å). Data reduction was made with the Bruker Saint program. The structures were solved by direct methods and refined with full-matrix least squares technique using the SHELXTL package. Non-hydrogen atoms were refined with anisotropic displacement parameters during the final cycles. Hydrogen atoms were placed in calculated positions with isotropic displacement parameters set to 1.2 × U_{eq} of the attached atom. The unit cell includes a large region of disordered solvent molecules, which could not be modeled as discrete atomic sites. We employed PLATON/SQUEEZE to calculate the diffraction contribution of the solvent molecules and, thereby, to produce a set of solvent-free diffraction intensities; structures were then refined again using the data generated. Crystal data and refinement conditions are shown in Table S1. The crystal data for HHU-3 and HHU-4 have been deposited in CSD database, and labeled as 1566591 and 1566592, respectively.

Table S1. Crystal data and structure refinement for **HHU-3** and **HHU-4**

Identification code	**HHU-3**	**HHU-4**
CDDC	1566591	1566592
Empirical formula	$C66\ H33\ Cu6\ N3\ O30$	$C66\ H30\ Cu6\ O33$
Formula weight	1729.25	1732.20
Temperature	293(2) K	140 (2) K
Wavelength	0.71073 Å	0.71073 Å
Crystal system	Orthorhombic	Orthorhombic
Space group	C m c 21	C m c m
Unit cell dimensions.	a = 24.600(2) Å α = 90°	a = 24.6748(11) Å α = 90°
	b = 33.412(3) Å β = 90°	b = 33.5109(15) Å β = 90°
	c = 18.478(2) Å γ = 90°	c = 18.4547(11) Å γ = 90°
Volume	15188(2) Å^3	15259.7 (13) Å^3
Z	4	4
Density (calculated)	0.756 g cm^{-3}	0.754 g cm^{-3}

Absorption coefficient	0.866 mm^{-1}	0.863 mm^{-1}
F(000)	3456	3456
Crystal size	0.2 x 0.1 x 0.1 mm	0.2 x 0.1 x 0.1 mm
Theta range for data collection.	2.01 to 26.41 °	2.29 to 25.00 °
Limiting indices	-20 <= h <= 30, -38 <= k <= 41, -23 <= l <= 22	-27 <= *h* <= 29, -39 <= *k* <= 39, -21 <= *l* <= 21
Reflections collected / unique	55146/15966 [R(int) = 0.1134]	100802/7128[R(int) = 0.1770]
Completeness	99.8 % (theta = 26.41°)	96.0 % (theta = 25.00°)
Absorption correction	Semi-empirical from equivalents	Semi-empirical from equivalents
Max. and min. transmission	0.917 and 0.901	0.917 and 0.901
Refinement method	Full-matrix least-squares on F^2	Full-matrix least-squares on F^2
Data /restraints / parameters	15966 / 43 / 485	6843 / 12 / 266
Goodness-of-fit on F^2	0.898	1.021
Final R indices [I>2sigma(I)]	R1^a = 0.0604, wR2 ^{a} = 0.1201	R1^a = 0.0751, wR2 ^{a} = 0.1828
R indices (all data)	R1 ^{a} = 0.1040, wR2 ^{a} = 0.1309	R1 ^{a} = 0.1500, wR2 ^{a} = 0.2111
Largest diff. peak and hole	0.607 and -0.345 e. Å^{-3}	0.956 and -0.681 e. Å^{-3}

[a] $R1 = \Sigma||F_o| - |F_c||/|F_o|$; $wR2 = [\Sigma w(\Sigma F_o^2 - F_c^2)^2/\Sigma w(F_o^2)^2]^{1/2}$.

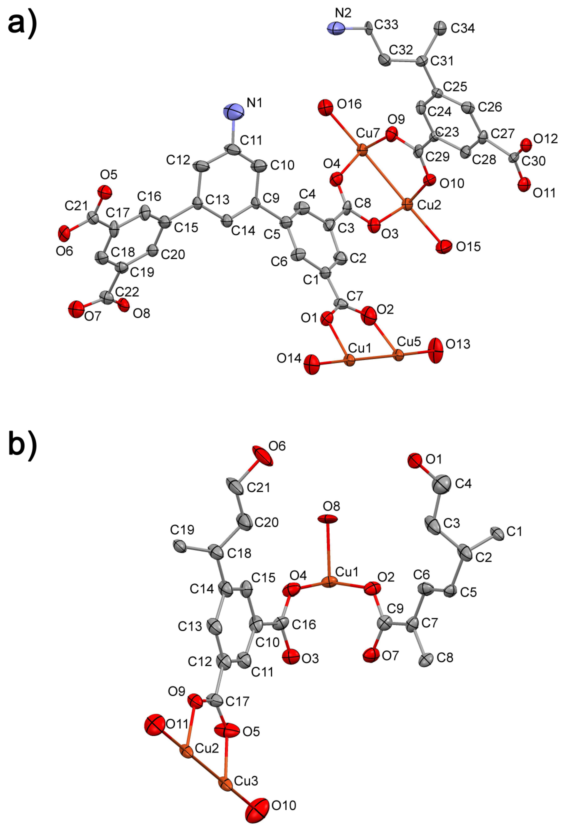

Figure S1 The asymmetric unit of HHU-3 (a) and HHU-4 (b).

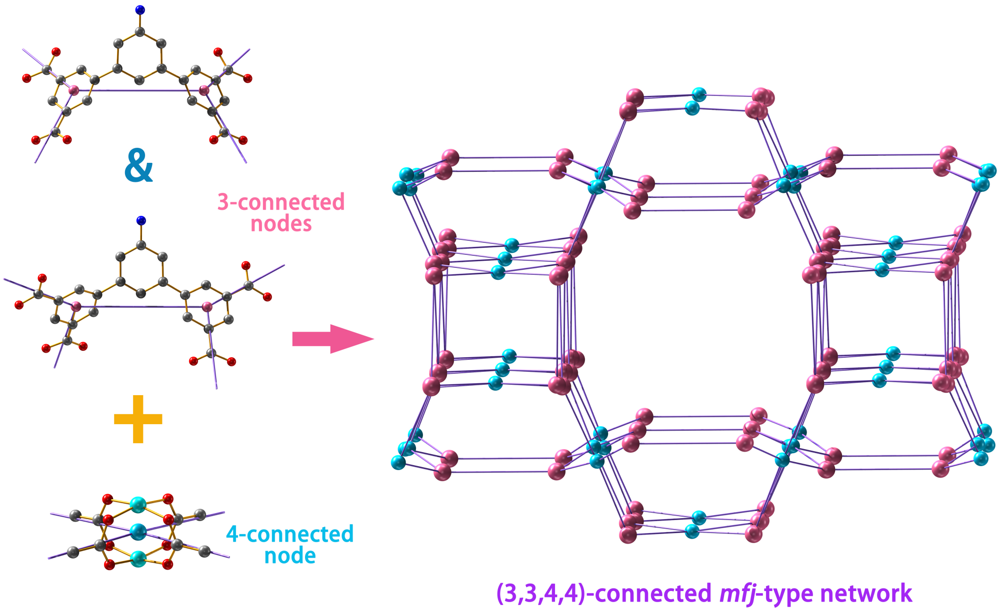

Figure S2 The topology simplification of HHU-3.

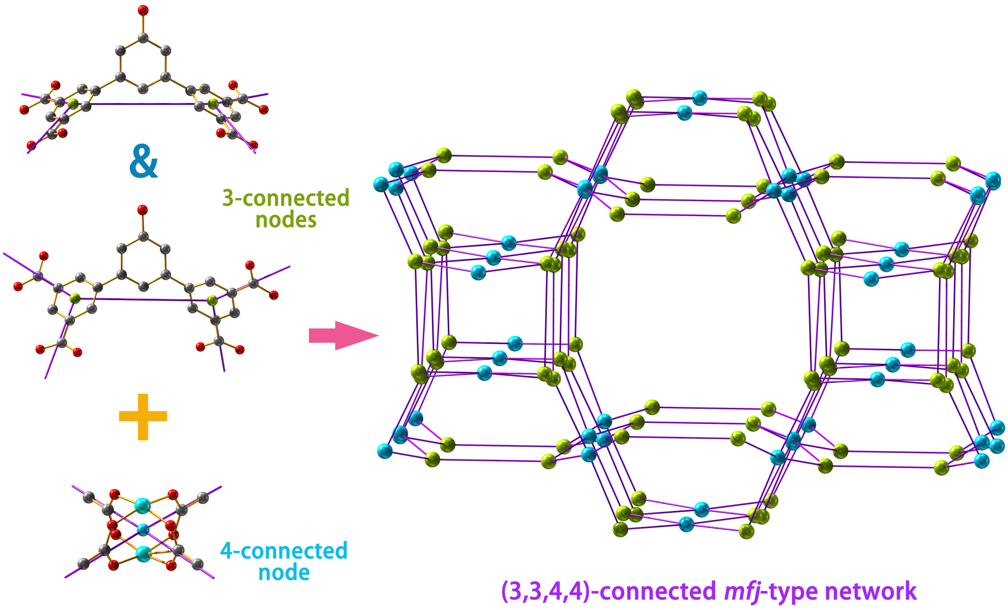

Figure S3 The topology simplification of HHU-4.

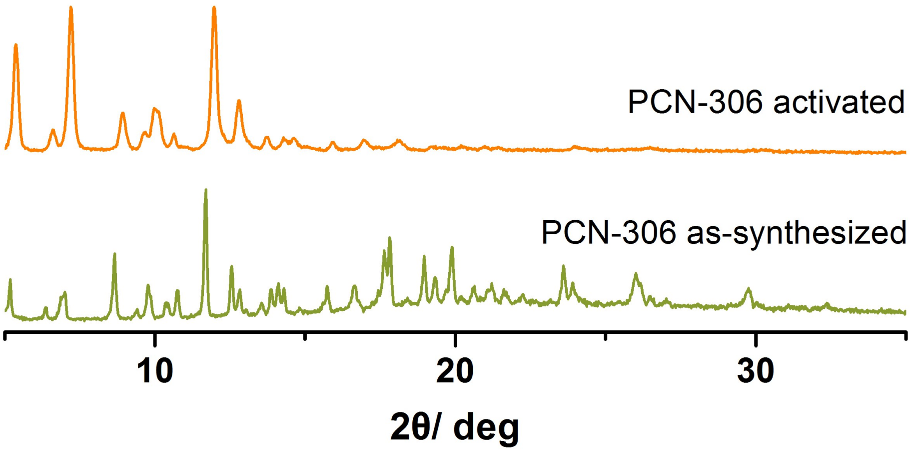

Figure S4 Powder X-ray diffraction (PXRD) patterns of PCN-306.

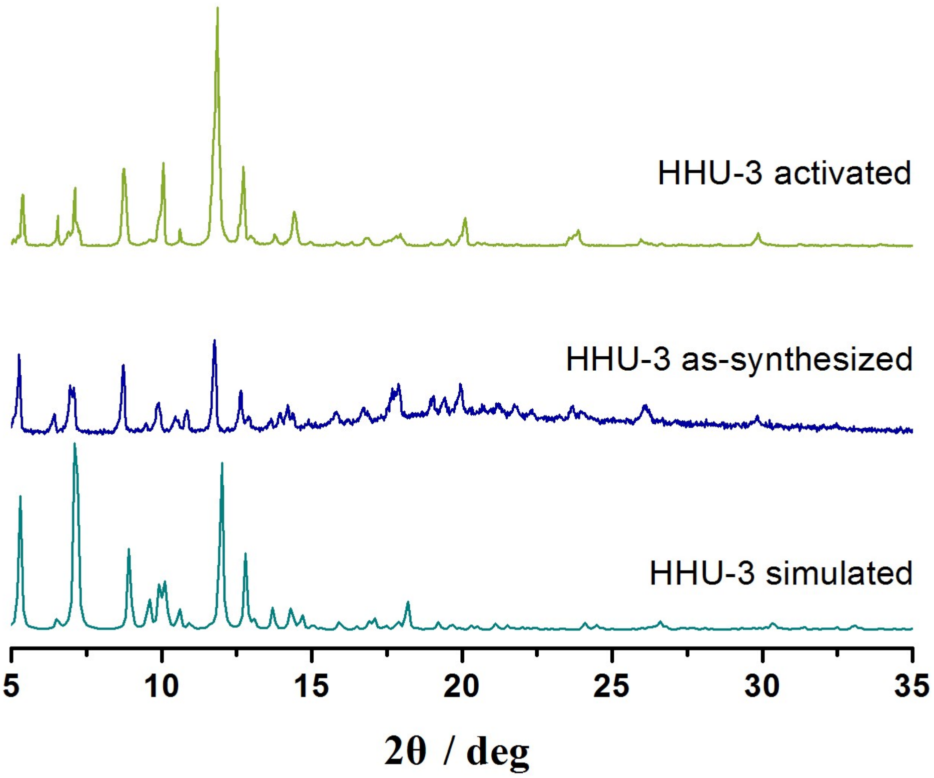

Figure S5 Powder X-ray diffraction (PXRD) patterns of HHU-3.

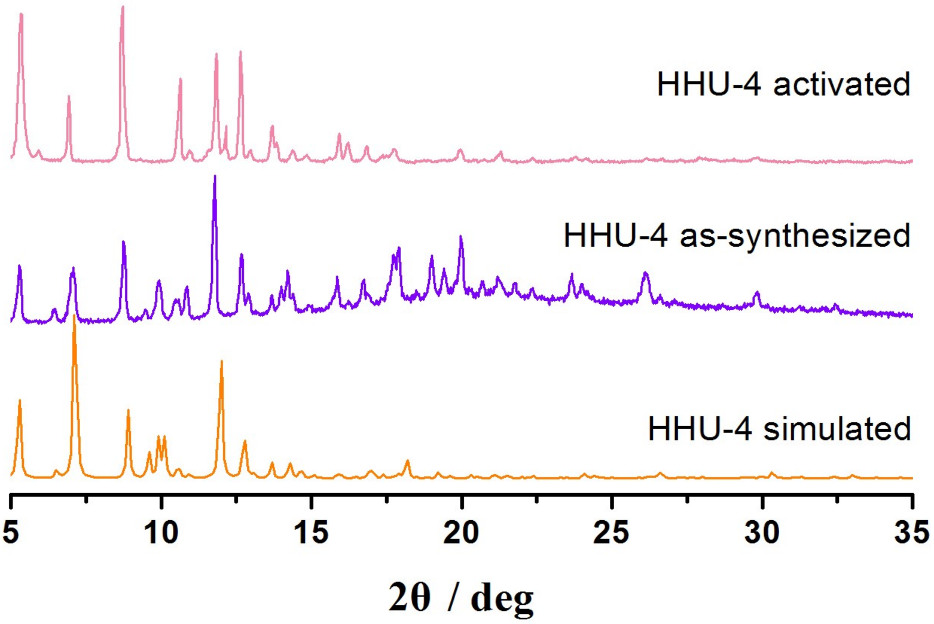

Figure S6 Powder X-ray diffraction (PXRD) patterns of HHU-4.

5. Low-Pressure Gas Sorption Measurements.

The N_2 (99.999 %) adsorption/desorption isotherms were measured volumetrically using a Micromeritics ASAP 2020 surface area and pore size analyzer up to saturated pressure at 77 K. Acetone or methanol-exchanged samples were charged into a sample tube and activated at corresponding temperature for 12 hours by using the "outgas" function of the surface area analyzer. The resulting mass of dried material was ~ 200 mg. Helium (99.999 %) was used for the estimation of the free space (dead volume), assuming that it is not adsorbed at any of the studied temperatures. To provide the relative pressure P/P_0 accurately at each data point, the saturation pressure P_0 was monitored and measured throughout the gases analyses by a dedicated saturation pressure transducer. The specific surface areas were determined using the Brunauer-Emmett-Teller (BET) and the Langmuir equation from the N_2 sorption data. When applying the BET theory, we made sure that our analysis satisfies the two consistency criteria as detailed by Walton and co-workers[1]. For the Langmuir surface areas, data from the whole adsorption data were used.

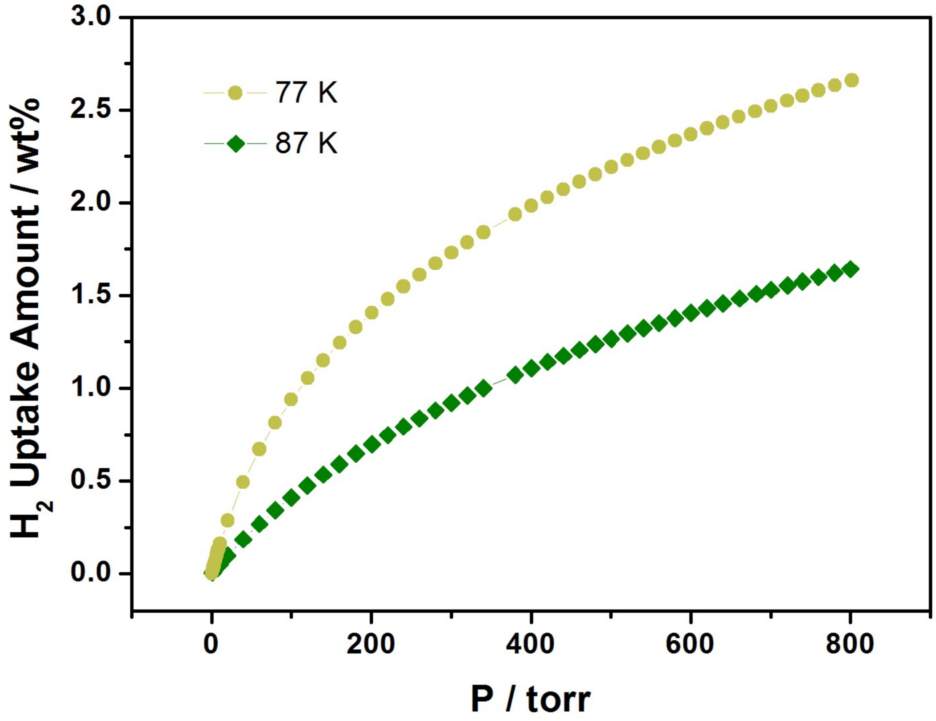

Figure S7 H_2 isotherms of PCN-306 at 77 K and 87 K.

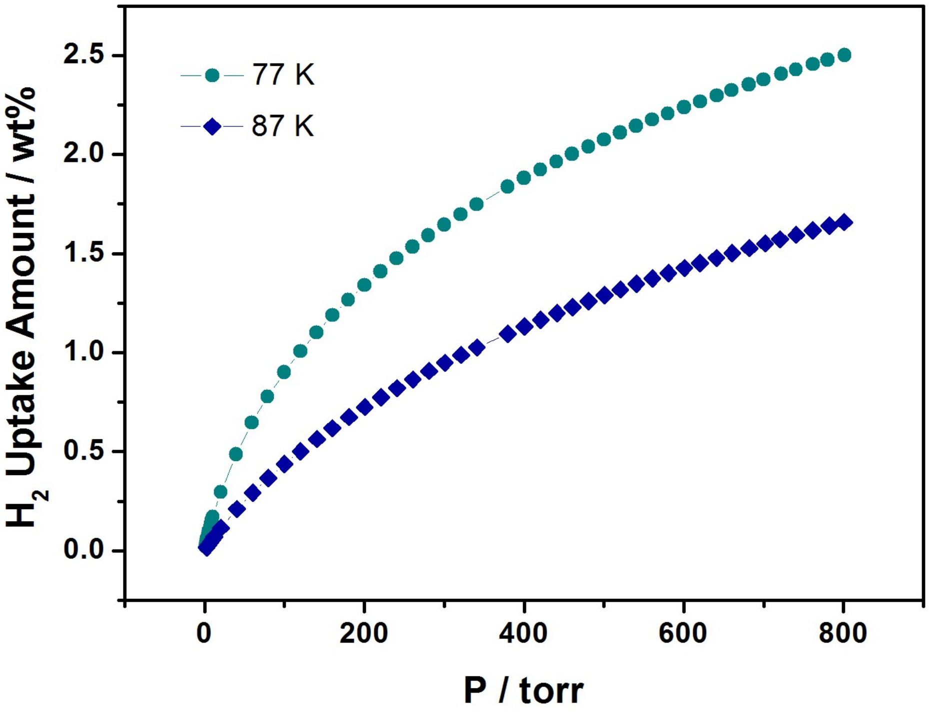

Figure S8 H_2 isotherms of HHU-3 at 77 K and 87 K.

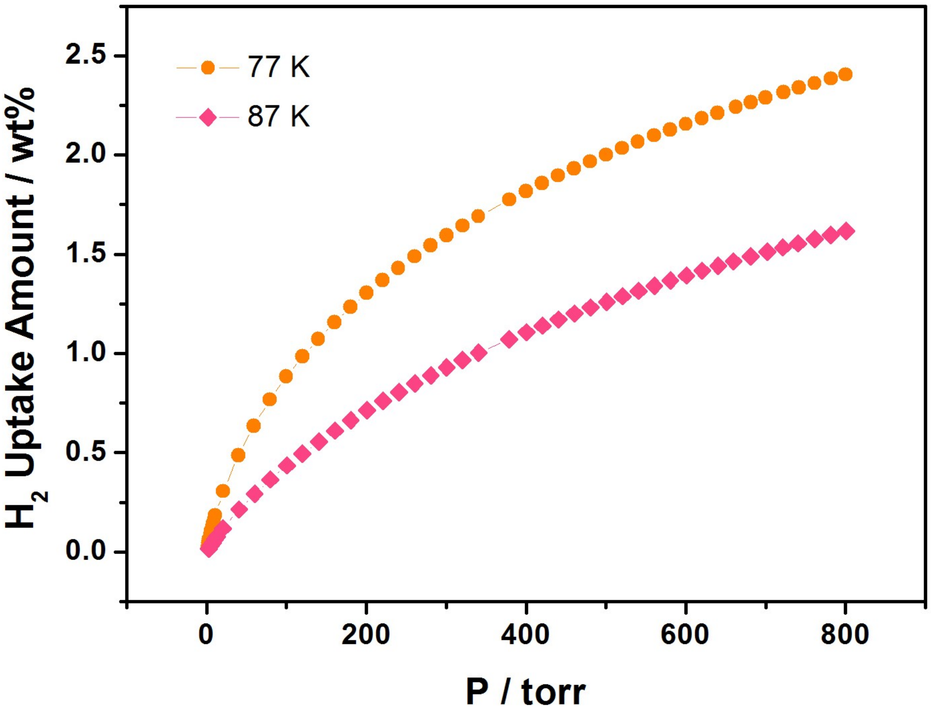

Figure S9 H_2 isotherms of HHU-4 at 77 K and 87 K.

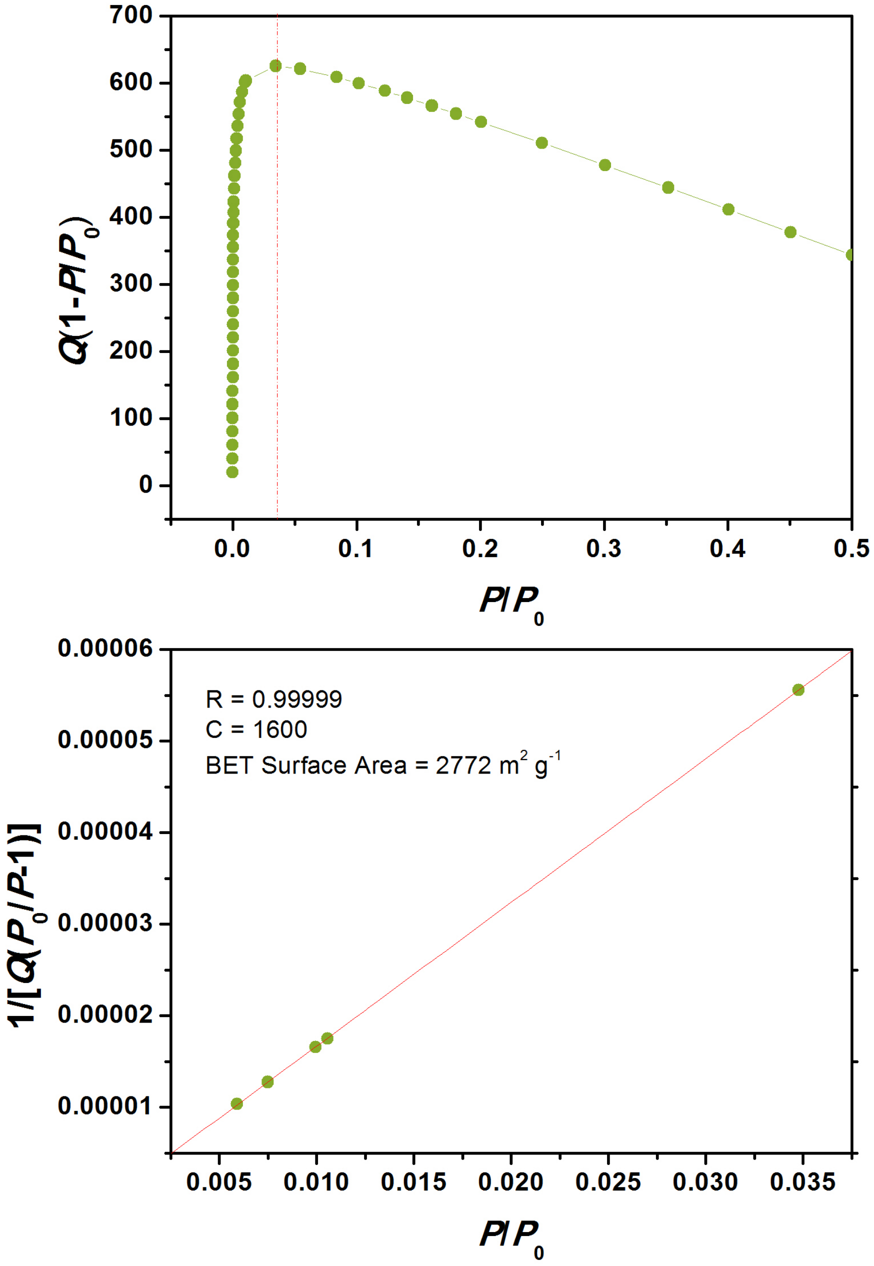

Figure S10 Top: $Q(1-P/P_0)$ vs. P/P_0 for simulated N_2 isotherm in PCN-306. Only the range below P/P0 = 0.035 satisfies the first consistency criterion for application of the BET theory. Bottom: Plot of the linear region for the BET equation, which satisfies the second criterion for application of the BET theory.

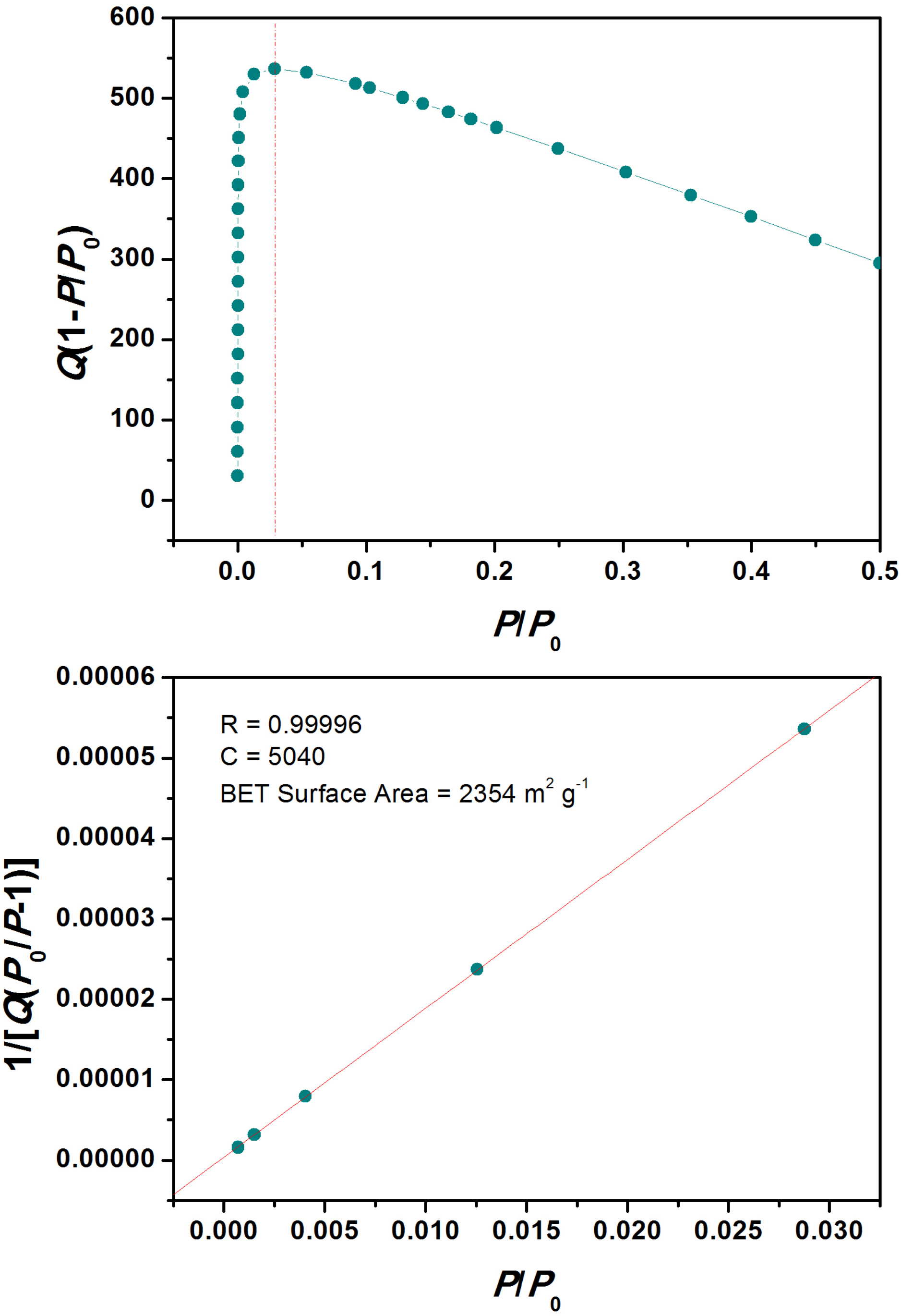

Figure S11 Top: $Q(1-P/P_0)$ vs. P/P_0 for simulated N_2 isotherm in HHU-3. Only the range below P/P0 = 0.03 satisfies the first consistency criterion for application of the BET theory. Bottom: Plot of the linear region for the BET equation, which satisfies the second criterion for application of the BET theory.

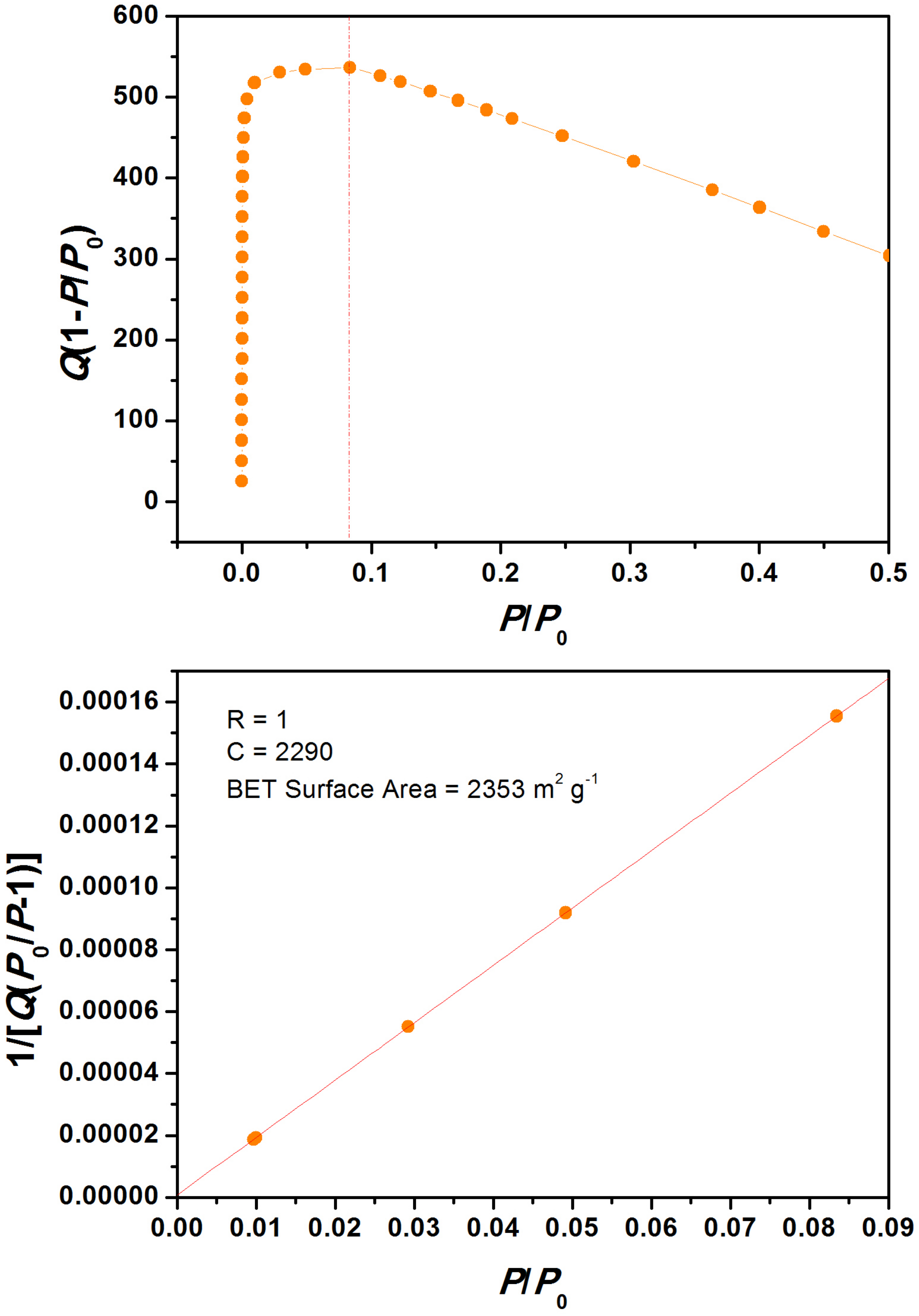

Figure S12 Top: $Q(1-P/P_0)$ vs. P/P_0 for simulated N_2 isotherm in HHU-4. Only the range below P/P0 = 0.085 satisfies the first consistency criterion for application of the BET theory. Bottom: Plot of the linear region for the BET equation, which satisfies the second criterion for application of the BET theory.

6. Calculating principle of gas loading

In the manuscript, the wt% gas uptake is defined as:

$$wt\% = \frac{100 \times N}{1000 + N} \tag{2}$$

7. Heats of Adsorption

A virial-type[2] expression comprising the temperature-independent parameters a_i and b_i was employed to calculate the enthalpies of adsorption for H_2 (at 77 and 87 K) and CO2 (at 273 K and 298 K) on **PCN-306, HHU-3, and HHU-4**. In each case, the data were fitted using the equation:

$$\ln P = \ln N + 1/T \sum_{i=0}^{m} a_i N^i + \sum_{j=0}^{n} b_j N^j \tag{4}$$

Here, P is the pressure expressed in Torr, N is the amount adsorbed in mmol/g, T is the temperature in K, a_i and b_j are virial coefficients, and m, n represent the number of coefficients required to adequately describe the isotherms (m and n were gradually increased until the contribution of extra added a and b coefficients was deemed to be statistically insignificant towards the overall fit, and the average value of the squared deviations from the experimental values was minimized). The values of the virial coefficients a_0 through a_m were then used to calculate the isosteric heat of adsorption using the following expression.

$$Q_{st} = -R \sum_{i=0}^{m} a_i N^i \tag{5}$$

Q_{st} is the coverage-dependent isosteric heat of adsorption and R is the universal gas constant.

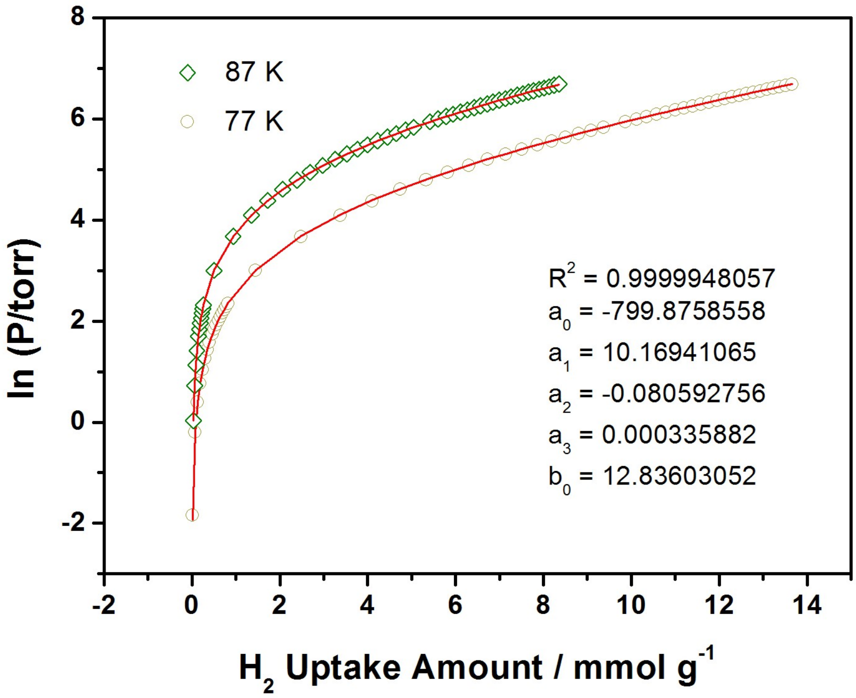

Figure S13 The details of virial equation (solid lines) fitting to the experimental H_2 adsorption data (symbols) for PCN-306.

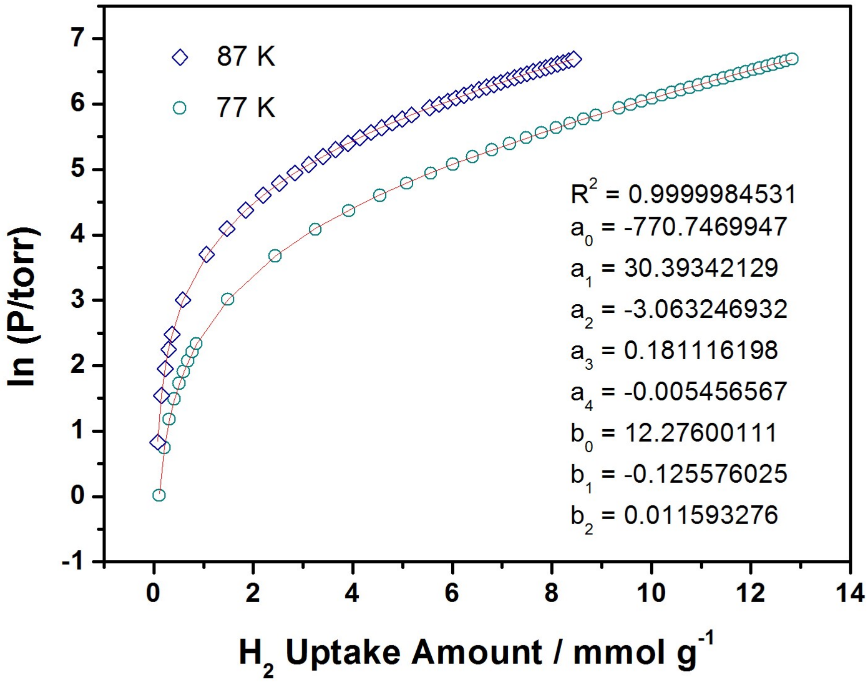

Figure S14 The details of virial equation (solid lines) fitting to the experimental H_2 adsorption data (symbols) for HHU-3.

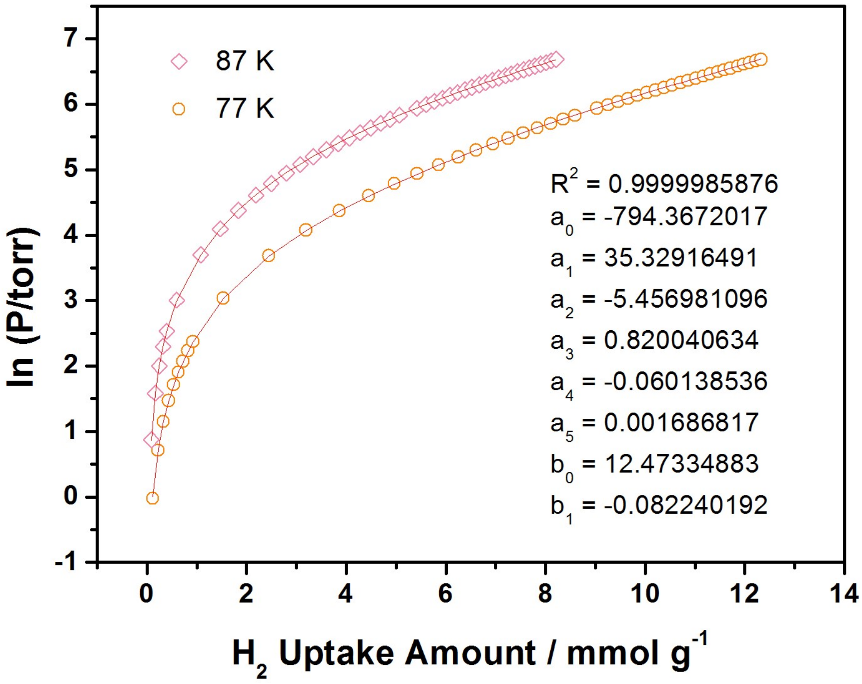

Figure S15 The details of virial equation (solid lines) fitting to the experimental H_2 adsorption data (symbols) for HHU-4.

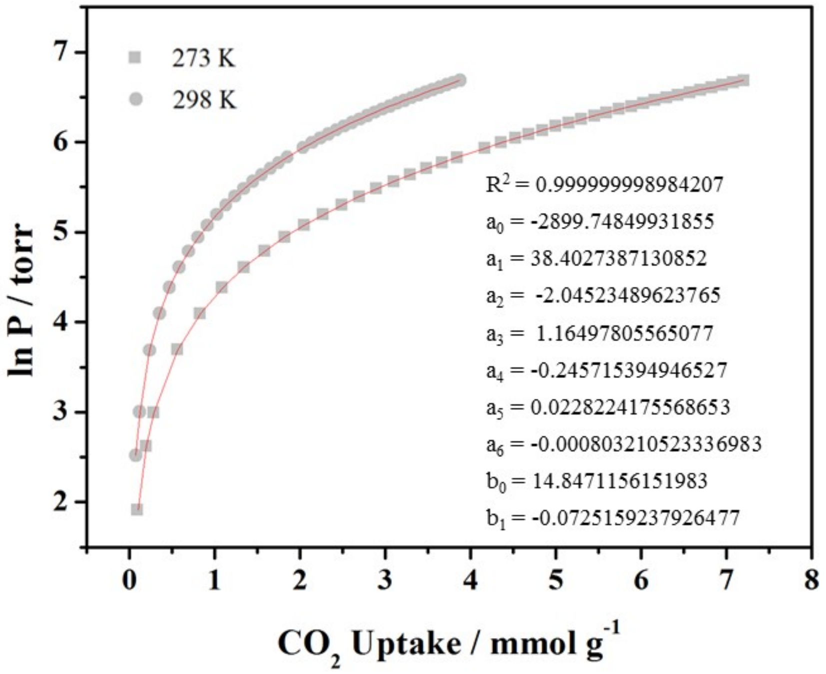

Figure S16 The CO_2 isotherms at 273 K and 298 K (symbols) and the virial equation fits (lines) for PCN-306.

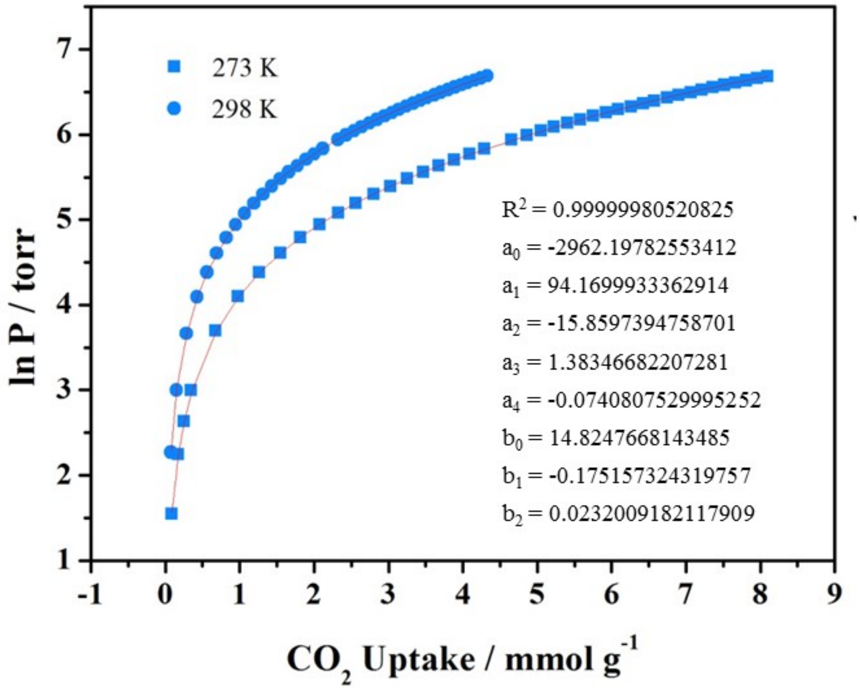

Figure S17 The CO_2 isotherms at 273 K and 298 K (symbols) and the virial equation fits (lines) for HHU-3.

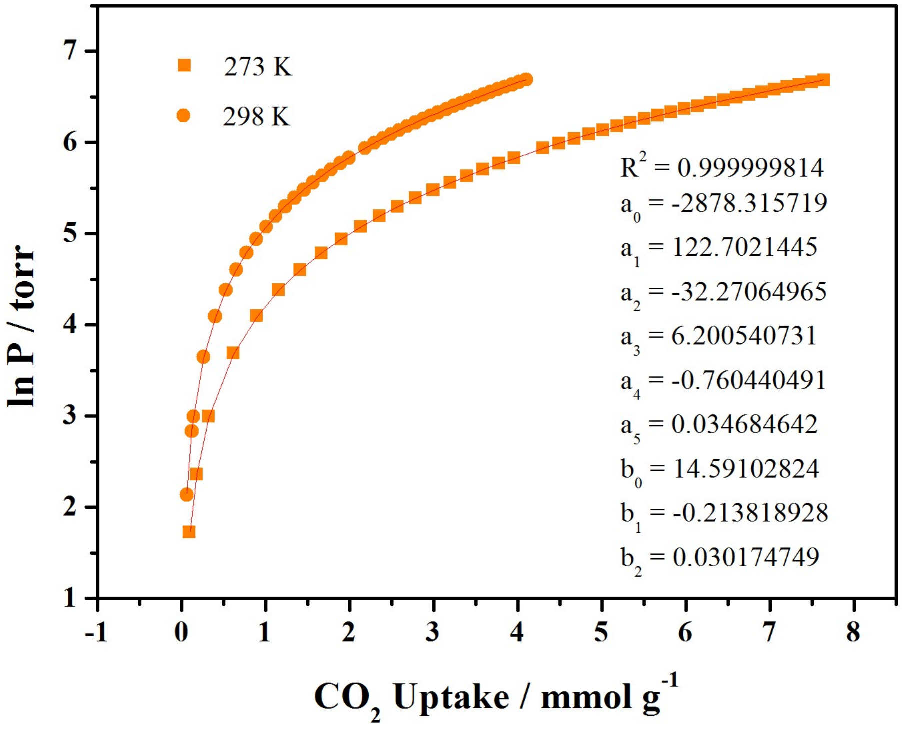

Figure S18 The CO_2 isotherms at 273 K and 298 K (symbols) and the virial equation fits (lines) for HHU-4.

8. Ideal Adsorbed Solution Theory (IAST) Calculated Selectivity.

IAST was used to predict binary mixture adsorption from the experimental pure-gas isotherms. In order to perform the integrations required by IAST, the single component isotherms should be fitted by a proper model. Usually the dual-site Langmuir-Freundlich equation is widely used in fitting the data:

$$q = q_{m1} \cdot \frac{b_1 \cdot P^{1/n_1}}{1 + b_1 \cdot P^{1/n_1}} + q_{m2} \cdot \frac{b_2 \cdot P^{1/n_2}}{1 + b_2 \cdot P^{1/n_2}}$$

Here, P is the pressure of the bulk gas at equilibrium with the adsorbed phase (kPa), q is the adsorbed amount per mass of adsorbent (mol/kg), qm1 and qm2 are the saturation capacities of sites 1 and 2 (mol/kg), b1 and b2 are the affinity coefficients of sites 1 and 2 (1/kPa), and n_1 and n_2 represent the deviations from an ideal homogeneous surface. The fitted parameters were then used to predict multi-component adsorption with IAST.

The selectivity $S_{A/B}$ in a binary mixture of components A and B is defined as $(x_A/y_A)/(x_B/y_B)$, where x_i and y_i are the mole fractions of component i (i = A, B) in the adsorbed and bulk phases, respectively.

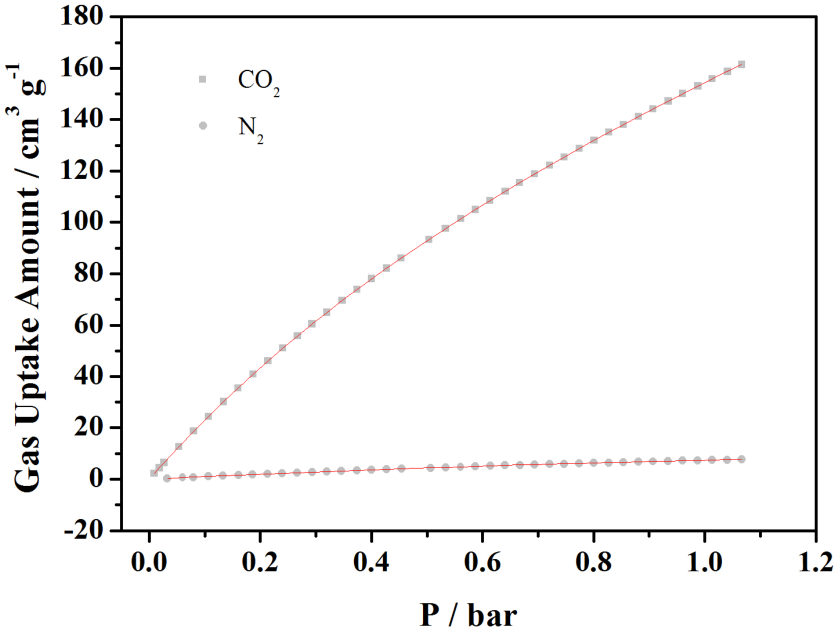

Figure S19 Comparison of experimental and simulated single-component isotherms of CO_2 and N_2 in PCN-306 at 273 K. The lines through the experimental data are fits to the dual-site Langmuir-Freundlich model.

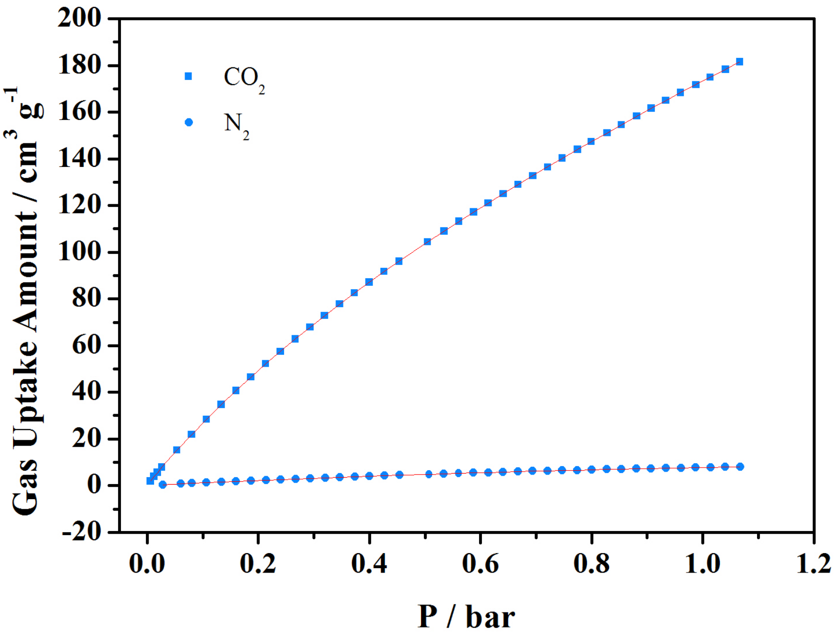

Figure S20 Comparison of experimental and simulated single-component isotherms of CO_2 and N_2 in HHU-3 at 273 K. The lines through the experimental data are fits to the dual-site Langmuir-Freundlich model.

9. Thermogravimetric analysis.

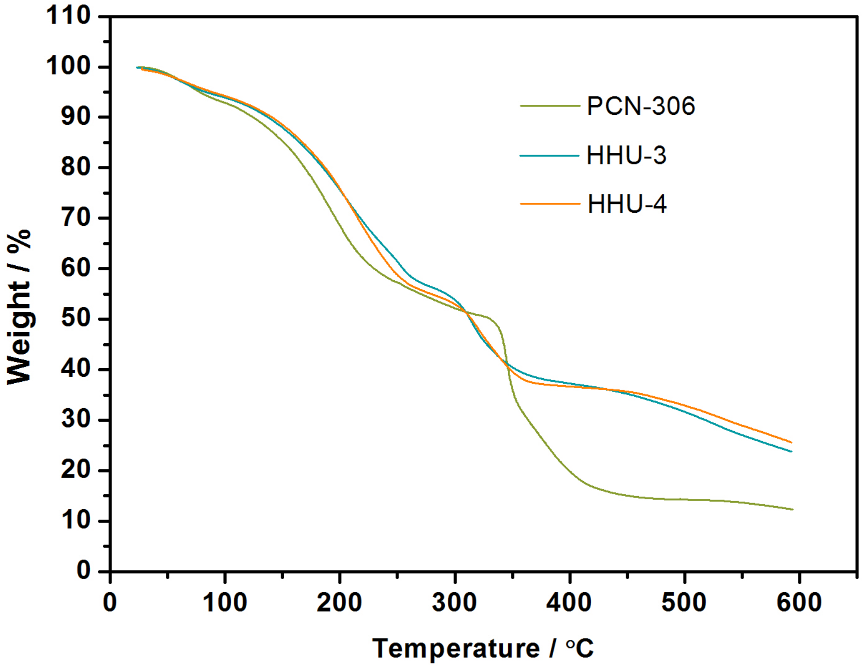

Figure S21 TGA curves of PCN-306, HHU-3, and HHU-4.

References:

[1] a) K. S. Walton and R. Q. Snurr, *J. Am. Chem. Soc.*, 2007, **129**, 8552; b) J. Rouquerol, P. Llewellyn and F. Rouquerol, *Stud. Surf. Sci. Catal.*, 2007, **160**, 49.

[2] J. L. C. Rowsell and O. M. Yaghi, *J. Am. Chem. Soc.*, 2006, **128**, 1304.